International Journal of Thermophysics, Vol. 18, No. 4, 1997

Application of the Linear Isotherm Regularity to Selected Fluid Systems[1]

S. Alavi[2]

Dense hard-sphere and Lennard–Jones fluids and also liquid mercury and water are studied to see if they obey the linear isotherm regularity suggested by Parsafar and Mason. For dense hard-sphere fluids a behavior consistent with the regularity is observed. Data from simulations of the Lennard–Jones fluid were observed to follow the trends proposed by the regularity. For mercury, agreement between the experimental data and the predictions of the regularity is obtained. This suggests that the scope of the regularity can be extended to include liquid metals. In the case of water, for pressure ranges that are not too large, quantitative agreement with the predictions of the regularity can be obtained. Over larger ranges of pressure, systematic deviations appear, but the agreement is still satisfactory. Based on the model previously proposed for the regularity, a discussion of some aspects of the parameters in the equation is given.

KEY WORDS: dense fluids; hard-sphere fluid; Lennard–Jones fluid; linear isotherm regularity; mercury; water.

1. INTRODUCTION

A general regularity has recently been reported for supercritical and subcritical dense fluids [1]. This regularity, which is equivalent to an equation of state, was shown to be valid for a wide range of fluids including nonpolar, polar, quantum, and weakly hydrogen-bonded fluids, as well as fluid mixtures [2]. With this equation of state, a number of previously known regularities were reproduced and some new regularities predicted, with physical interpretations given for each case [3]. Selected thermophysical properties were also studied [4].

[1] Paper dedicated to Professor Edward A. Mason.

[2] Department of Chemistry, University of British Columbia, Vancouver, British Columbia V6T 1Z1, Canada.

0195-928X/97/0700-1035$12.50/0 © 1997 Plenum Publishing Corporation

The regularity states that isotherms of $(Z-1)\,v^2$ are linear with ρ^2,

$$(Z-1)\,v^2 = A + B\rho^2 \tag{1}$$

where $Z = pv/RT$ is the compressibility factor and $\rho = 1/v$ is the molar density of the fluid. A and B are parameters with a temperature dependence given by

$$A = A_2 - A_1/RT \tag{2}$$

and

$$B = B_1/RT \tag{3}$$

where A_2, A_1, and B_1 are constants depending on the nature and composition of the dense fluid.

The regularity was noticed to be valid for densities larger than the Boyle density and temperatures from the triple point to approximately twice the Boyle temperature. This includes most of the liquid region and regions of the dense supercritical fluid near the solid phase of the phase diagram.

In this paper, a number of fluid systems not studied previously are examined to see if they can be incorporated into the scheme of the regularity. These systems are hard-sphere and Lennard–Jones fluids, mercury, and water.

2. SUMMARY OF THE MODEL

For completeness, a summary of the model proposed to mimic the linearity of $(Z-1)\,v^2$ against ρ^2 is given. Further details are provided in Ref. 1.

The starting point is the thermodynamic equation of state,

$$p = T\left(\frac{\partial p}{\partial T}\right)_v - \left(\frac{\partial E}{\partial V}\right)_T \tag{4}$$

where $T(\partial p/\partial T)_v$ is the thermal pressure and $(\partial E/\partial V)_T$ the internal pressure of the fluid.

To obtain an expression for the internal pressure, a simple model of the internal energy of the system is used. It is assumed that the kinetic energy is independent of the volume and thus does not contribute to the internal pressure. The potential energy of the system is taken to consist of only pairwise additive nearest-neighbor interactions, with the number of

nearest neighbors being proportional to the density of the fluid. In order to obtain the isotherm regularity given by Eq. (1), the pair interaction was required to have the form of $C_9/r^9 - C_3/r^3$. Substituting these results into the thermodynamic equation of state and rearranging, one obtains

$$(Z-1)\,v^2 = -\frac{A_1}{RT} + \frac{B_1}{RT}\rho^2 + \frac{1}{\rho^2}\left[\frac{1}{\rho R}\left(\frac{\partial p}{\partial T}\right)_\rho - 1\right] \tag{5}$$

A_1 and B_1 are related, respectively, to the contributions of attraction and repulsion to the internal pressure, and the final term on the right is the nonideal contribution to the thermal pressure. It was argued that this term is slowly varying for Ar in the density range of interest. The corresponding term for the van der Waals equation, $b/[\rho(1-b\rho)]$, gives an indication of why this should be so. This term becomes infinite at low densities where $\rho \to 0$, and at high densities as $b\rho \to 1$, but is a slowly varying function at intermediate values, especially near the minimum, $b\rho = 1/2$. If this term is taken to be constant and designated by A_2, Eq. (1) is obtained.

The insensitivity of the linearity to the form of the pair potential is not apparent from this model but is indicated from studies of the predictions of the van der Waals and the accurate Ihm–Song–Mason equations of state, each of which is based on different models for effective intermolecular potentials [5, 6]. Thus it is seen that the linearity arises as a result of the balance of attractive and repulsive forces in the density and temperature range of interest and is not sensitive to the particular form of the forces. This illustrates why the regularity should hold for such a variety of fluids despite their widely different intermolecular potentials.

3. HARD-SPHERE FLUID

The Carnahan–Starling equation of state gives an essentially exact representation of hard-sphere fluid behavior over the entire range of fluid densities [7]. In terms of the molar density, this equation is given by

$$Z = \frac{1 + \alpha\rho + (\alpha\rho)^2 - (\alpha\rho)^3}{(1-\alpha\rho)^3} \tag{6}$$

where $\alpha = \pi d^3 N_A/6$, N_A being Avogadro's number and d the molecular diameter.

It is not obvious that this equation can be rearranged to give that $(Z-1)\,v^2$ is linear with ρ^2. On the other hand, from the point of view of the model stated in Sect. 2, the linearity of $(Z-1)\,v^2$ against ρ^2 isotherms is a result of the balance of attractive and repulsive forces. In a hard-sphere

fluid there are no two body attractions, but due to the presence of a potential of mean force, an effective attraction between two molecules may be seen. Thus it may be possible to find behavior consistent with Eq. (1).

In a hard-sphere fluid, as in the general case of Sect. 2, the kinetic energy is assumed to be independent of volume. The potential energy is also independent of volume in this case, and $(\partial E/\partial V)\,T=0$ for a hard-sphere fluid. Therefore, in the thermodynamic equation of state, deviations from ideality arise from nonideal contributions to the thermal pressure. For hard-spheres Eq. (5) is thus given by

$$(Z-1)\left(\frac{v}{\alpha}\right)^2=\frac{1}{(\alpha\rho)^2}\left[\frac{1}{\rho R}\left(\frac{\partial p}{\partial T}\right)_\rho-1\right]=\frac{4-2\alpha\rho}{\alpha\rho(1-\alpha\rho)^3} \tag{7}$$

As mentioned, for Ar and the van der Waals equation, the nonideal contribution to the thermal pressure is relatively constant in the range of density and temperature which the linear regularity holds. Equation (7) is plotted in Fig. 1. It can be seen that the resulting function is relatively constant in the intermediate density region, in the vicinity of the minimum [at $(\alpha\rho)^2\approx 0.078$].

Hard-spheres have only one fluid phase and have no Boyle temperature. The closest packing density for hard spheres lies at $\alpha\rho=0.74$ [$(\alpha\rho)^2=0.55$] and crystallization for a hard-sphere fluid occurs at $\alpha\rho=0.49$ [$(\alpha\rho)^2=0.25$]

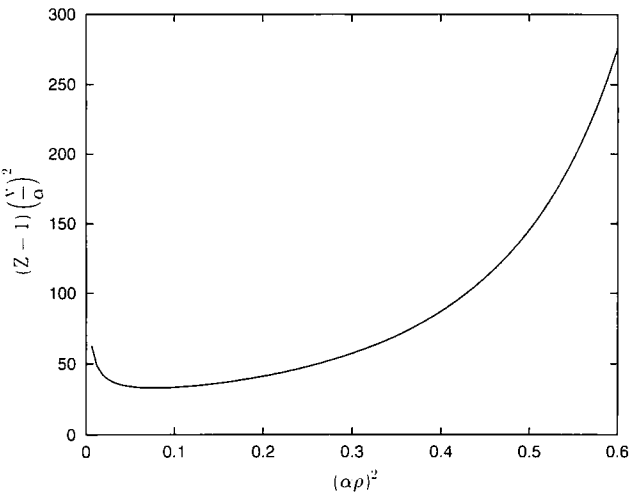

Fig. 1. Reduced nonideal thermal pressure of a hard-sphere fluid as a function of the square of the reduced molar density.

[8]. Therefore, in a limited dense fluid region of $(\alpha\rho)^2 = 0.05$ to 0.2, a reasonable approximation for a hard-sphere fluid would be

$$(Z-1)\,v^2 = A_2 \tag{8}$$

where A_2 is a positive temperature-independent constant representing the nonideal contribution to the thermal pressure.

The behavior of $(Z-1)\,v^2$ against ρ^2 for hard spheres, shown in Fig. 1, is comparable to the high-temperature behavior of the same function for the van der Waals and Ihm–Song–Mason equations, as shown in Figs. 7 and 8 of Ref. 1, where, due to repulsion, $(Z-1)\,v^2$ has divergences at the high and low density limits, but at intermediate densities a region of relative constancy is seen. Equation (5) shows that at high temperatures, nonideal thermal pressure effects will dominate over internal pressure effects, and so these systems will show similar behavior.

4. LENNARD–JONES FLUID

At temperatures that are not too low, argon is considered to a good approximation to be a Lennard–Jones fluid [8]. Thus it is reasonable to expect that like argon, Lennard–Jones fluids will follow the linear isotherm regularity. Simulation results for Lennard–Jones fluids are available and this assumption can be studied directly. Moreover, simulations may extend into regions where experimental data are difficult to obtain or nonexistent.

The phase diagram of the Lennard–Jones fluid is known [8]. The critical temperature and density of the Lennard–Jones fluid are at $T_c^* = 1.36$ and $\rho_c^* = 0.36$, where $T^* = kT/\varepsilon$ and $\rho^* = N\sigma^3/V$. The triple-point temperature and density are $T_{tp}^* = 0.68 \pm 0.02$, and $\rho_{tp}^* = 0.85 \pm 0.01$. The Boyle temperature and density of a Lennard–Jones fluid may be obtained from Hirschfelder et al. [9]. The values are $T_B^* = 3.42$ and $\rho_B^* = 0.4$.

Some values of reduced pressure and density of a Lennard–Jones *liquid* have been given for selected isotherms by McDonald and Singer [10]. A number of these isotherms are plotted as $(Z-1)(v^*)^2$ against $(\rho^*)^2$ in Fig. 2. Good linearity is obtained and the random deviations observed are likely due to simulation results. The temperature dependence of the slopes and intercepts can be obtained and are represented to a good extent by Eqs. (2) and (3).

Simulation results [11, 12] for $(Z-1)(v^*)^2$ against $(\rho^*)^2$ isotherms from $T^* = 0.75$ to $T^* = 100$ are shown in Fig. 3. The high-density regions of the curves extend to about the freezing line (the full extent of the two high-temperature isotherms has not been shown), and both subcritical and supercritical temperatures are included. At low densities, the low-tem-

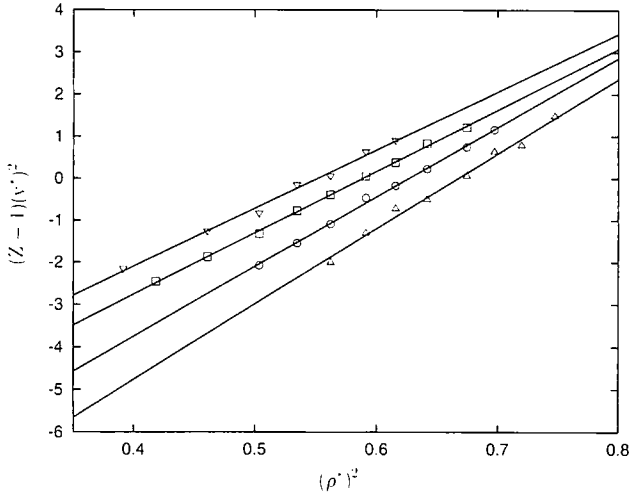

Fig. 2. Isotherms of $(Z-1)(v^*)^2$ against $(\rho^*)^2$ for Lennard–Jones liquid using data of Ref. 10. Isotherms correspond to reduced temperatures T^* of 0.902 (△), 0.977 (○), 1.060 (□), and 1.135 (▽).

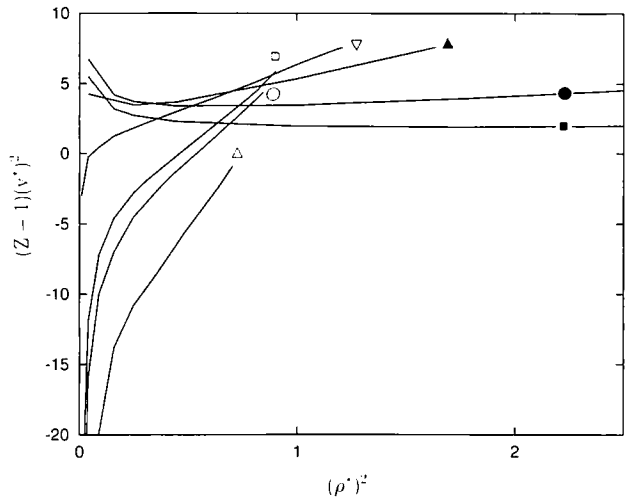

Fig. 3. Subcritical and supercritical isotherms for the Lennard–Jones fluid from Refs. 11 and 12. The reduced temperatures are 0.75 (△), 1.15 (○), 1.35 (□), 2.74 (▽), 5 (▲), 20 (●), and 100 (■).

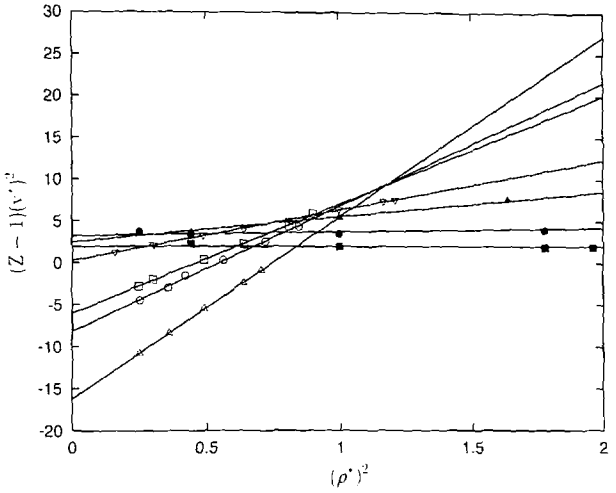

Fig. 4. Linear sections of Fig. 3. Simulation results are shown on each isotherm.

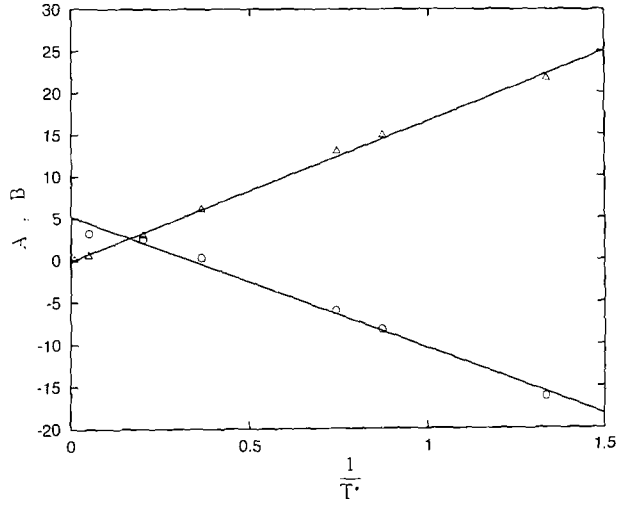

Fig. 5. Temperature dependence of the reduced slope B (△) and intercept A (○) parameters for the Lennard-Jones fluid.

perature isotherms diverge to negative values. For high-temperature isotherms, the low-density behavior indicates a divergence to positive values. This behavior is consistent with that of the van der Waals and Ihm–Sing–Mason equations of state discussed in Ref. 1.

The linear regions of the curves in Fig. 3, where densities are higher than the Boyle density are plotted separately in Fig. 4. The fit of the points to the lines does not meet the standard set in Ref. 1 of $r^2 \geqslant 0.995$, with r being the correlation coefficient, but this may again be related to random errors in simulation results and the small number of points available for each isotherm. In Ref. 1, it was stated that the linearity is valid for $\rho > \rho_B$ and $T < 2T_B$. The range of densities for which the linearity is valid for the Lennard–Jones fluid agrees with this range, but qualitatively at least, it appears that the linearity holds for a even larger range of temperatures.

The slopes and intercepts of the lines in Fig. 4, along with their one standard deviation error limits, are given in Table I. These values are plotted against $1/T^*$ in Fig. 5, and they can be seen to confirm to Eqs. (2) and (3). The approximate zero slope of the highest-temperature curve in Fig. 4 and, hence, the approximate zero intercept of the slope parameter are predicted by Eq. (3).

5. MERCURY

The linearity of isotherms of liquid metals was not studied in previous work. With the data of Grindley and Lind [13] for liquid mercury, $(Z-1)(v/v_c)^2$ was plotted against $(\rho/\rho_c)^2$ for different isotherms in Fig. 6. The

Table I. Reduced Intercept A and Slope B Parameters of $(Z-1)(v^*)^2 = A + B(\rho^*)^2$ for a Lennard-Jones Fluid

kT/ε	A	B	$\Delta\rho^{*a}$
0.75[b]	-16.24 ± 0.06	21.7 ± 0.1	0.017–0.23
0.902[c]	-11.9 ± 0.4	17.8 ± 0.7	0.807–1.644
0.977[c]	-10.4 ± 0.2	16.5 ± 0.3	0.031–1.476
1.060[c]	-8.60 ± 0.09	14.6 ± 0.2	0.019–1.582
1.135[c]	-7.6 ± 0.2	13.8 ± 0.4	0.112–1.386
1.15[b]	-8.2 ± 0.2	14.9 ± 0.3	0.070–4.99
1.35[b]	-6.0 ± 0.1	13.0 ± 0.2	0.097–8.10
2.74[b]	0.28 ± 0.03	6.04 ± 0.04	0.266–30.65
5[b]	2.5 ± 0.2	3.0 ± 0.2	1.17–34.38
20[b]	3.2 ± 0.2	0.5 ± 0.1	5.08–588.8
100[b]	1.9 ± 0.1	0.07 ± 0.02	24.4–4072

[a] The reduced pressure range for the data.
[b] From Refs. 11 and 12.
[c] From Ref. 10.

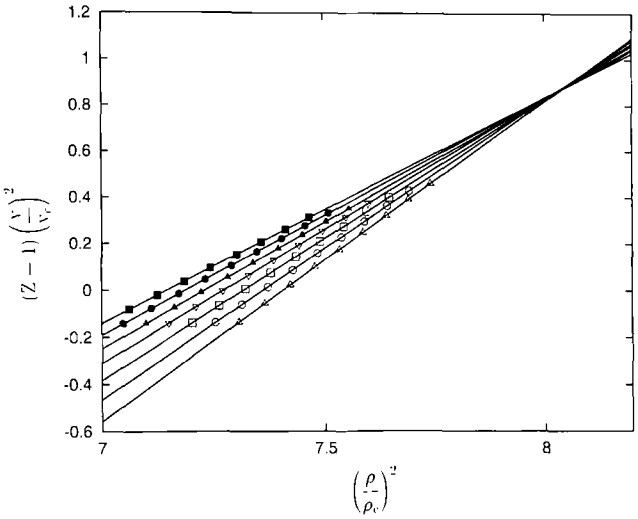

Fig. 6. $(Z-1)(\rho/\rho_c)^2$ against $(\rho/\rho_c)^2$ isotherms for mercury. The temperatures of the isotherms are 30°C (△), 50°C (–), 70°C (□), 90°C (▽), 110°C (▲), 130°C (●), and 150°C (■). Data are from Ref. 13.

pressures here range from 0 to 8000 bar. The slopes and intercepts of the lines, along with their one standard deviation error limits are given in Table II. Good linearity is obtained in the range given, and the prediction of the linear isotherm regularity that all isotherms will pass through a common compressibility factor point [3] is also seen to hold. From Fig. 6 this common point is at $(\rho/\rho_c)^2_{\text{exp.}} = 8.05$ and the prediction given from the

Table II. Reduced Intercept A and Slope B Parameters of $(Z-1)(\rho/\rho_c)^2 = A + B(\rho/\rho_c)^2$ for Liquid Mercury[a]

T(°C)	A	B	$(\lvert\Delta p\rvert)/p)\,100$[b]
30	10.18 ± 0.01	1.374 ± 0.001	1.6 (3.4)
50	9.50 ± 0.01	1.290 ± 0.001	1.6 (3.4)
70	8.861 ± 0.009	1.211 ± 0.001	1.6 (3.3)
90	8.314 ± 0.009	1.143 ± 0.001	1.6 (3.3)
110	7.80 ± 0.01	1.080 ± 0.001	1.6 (3.2)
130	7.36 ± 0.02	1.025 ± 0.002	1.6 (3.2)
150	6.95 ± 0.01	0.973 ± 0.002	1.6 (3.2)

[a] The pressure range is 0 to 8000 bar in all cases. Data are from Ref. 13.

[b] Absolute average percentage error in density at each temperature, along with the maximum error.

slopes and intercepts of the isotherms is $(\rho/\rho_c)^2_{calc.} = A_1/B_1\rho_c^2 = 8.06 \pm 0.04$ [3], an agreement within 0.1%. This is an indication of the accuracy of the representation of the temperature dependences of the slope and intercept by Eqs. (2) and (3).

The absolute average percentage error in the densities at different temperatures is also given in Table II. This error is 1.6% for the temperatures studied. In all isotherms, the largest deviation was related to the highest pressure (8000 bar).

6. WATER

In Fig. 7, the data of Grindley and Lind [13] have been used to plot a number of $(Z-1)(v/v_c)^2$ isotherms for liquid water against $(\rho/\rho_c)^2$. The range of pressures is again from 0 to 8000 bar. The isotherms show a degree of linearity, but systematic deviations from the straight line can be seen. Depending on the accuracy required, the representation of water data as $(Z-1)(v/v_c)^2$ linear against $(\rho/\rho_c)^2$ can be considered as a satisfactory approximation. The correlation coefficient of the isotherms can be increased by using a smaller range of pressure in the plot. Thus in a more limited range of pressure, quantitative agreement can be obtained.

Because of the systematic deviations in the isotherms, extrapolations of the lines do not meet at a single point as predicted by the common com-

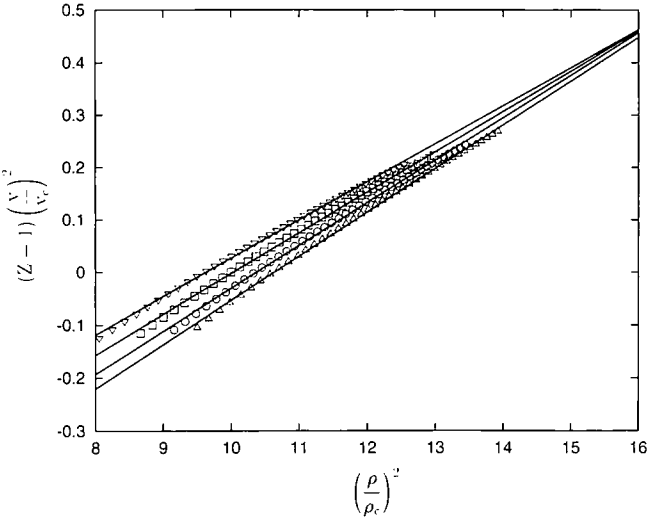

Fig. 7. $(Z-1)(v/v_c)^2$ against $(\rho/\rho_c)^2$ isotherms for water. The temperatures of the isotherms are 30°C (△), 70°C (○), 110°C (□), and 150°C (▽). Data are from Ref. 13.

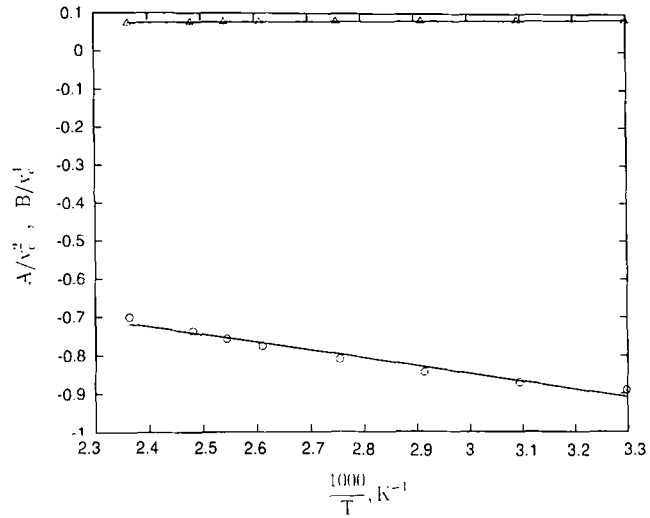

Fig. 8. Temperature dependence of the reduced slope B/v_c^4 (△) and reduced intercept A/v_c^2 (○) parameters for water.

pressibility factor regularity, but over some region. The prediction from the slope and intercept parameters for the common compressibility point is still reasonable.

The slopes and intercepts of the isotherms of water at different temperatures, along with their one standard deviation error limits, are given in Table III. The temperature dependence of the slope and intercept parameters are plotted in Fig. 8. The linearity is satisfactory in both cases and the intercept of the slope parameter is close to zero.

Table III. Reduced Intercept A and Slope B Parameters of $(Z-1)(v/v_c)^2 = A + B(p/p_c)^2$ for Liquid Water[a]

T (°C)	A	B
30	0.890 ± 0.005	0.0837 ± 0.0004
50	0.871 ± 0.005	0.0828 ± 0.0005
70	0.844 ± 0.006	0.0814 ± 0.0005
90	0.811 ± 0.005	0.0794 ± 0.0005
110	0.776 ± 0.005	0.0773 ± 0.0005
130	0.738 ± 0.004	0.0750 ± 0.0004
150	0.701 ± 0.004	0.0727 ± 0.0004

[a] The pressure range is 0 to 8000 bar in all cases. Data are from Ref. 13.

7. PARAMETERS IN THE EQUATION

It appears that, to an extent, writing the equation of state of dense fluids in the form of Eq. (1) eliminates individual peculiarities of fluids. Thus a wide range of dense fluids, from nonpolar, polar, quantum, metallic fluids, and even water, is satisfactorily described by a single equation of state.

Providing a more rigorous theoretical basis for this equation still remains a challenge. Further affirmation of the general aspects of the proposed model can be obtained from studying the magnitudes of A_1, A_2, and B_1 for different fluids and comparing these with the values expected from the physical interpretation given for the parameters.

The A_2 parameter represents the nonideal contribution to the thermal pressure in Eq. (5). As stated, this function is given for the van der Waals equation by $b/[\rho(1-b\rho)]$ and is relatively constant near the minimum. For the Carnahan–Starling equation this function was given by Eq. (7), which, as shown in Fig. 1, is again relatively constant in the vicinity of the minimum. For the van der Waals fluid, the value of A_2 at the minimum is $4b^2$, and for the Carnahan–Starling equation it is $32.9\alpha^2$, and, thus, proportional to d^6. In both cases, we get a squared excluded volume correlation for A_2 in the vicinity of the constant region, and it is reasonable to expect that for other fluids, this squared correlation with excluded volume will also hold.

In Ref. 1, the intermolecular potential was written as $(C_n/r^n - C_m/r^m)$. After some manipulation, C_m, and C_n are ultimately related to A_1 and B_1, respectively. Thus by comparing A_1 and B_1 parameters for different fluids, one may obtain some indication of the relative magnitudes of their intermolecular potential parameters. Considerations of the relative number of nearest neighbors will complicate this relation. This aspect of the parameters is implied in obtaining mixing and combination rules for mixtures [14]. A detailed study of the excluded volume correlation of A_2 and comparison of A_1 and B_1 parameters of different fluids will remain for future work.

The comparison of the magnitudes of A_1 and B_1 in each fluid leads to an interesting observation. One has

$$\frac{A_1}{B_1} \approx \frac{C_m}{C_n} \tag{9}$$

which is of interest when considering the nature of the attractions and repulsions in a fluid. A special case is the Lennard–Jones fluid, for which the potential is $4\varepsilon[(\sigma/r)^{12} - (\sigma/r)^6]$ and $C_m/C_n = 1$, when the distance is

expressed in reduced form, i.e., r/σ. From the simulations which gave the data in Figs. 2 and 4, two sets of A_1 and B_1 parameters can be obtained. In the absence of random differences in simulation results, these values should of course be the same. For the data of Fig. 2, the ratio A_1/B_1 is 1.1 ± 0.1, and for Fig. 4, the ratio is 0.92 ± 0.05. Both series of values for the Lennard–Jones fluid confirm the relation to a good extent. In Fig. 5, this aspect is indicated by the approximately equal magnitudes of the slopes of the two lines.

When the molar volume v is reduced with the critical molar volume v_c, it is straightforward to show that for a Lennard–Jones potential (or any inverse power potential whose repulsion and attraction differ by a six powers of r), Eq. (9) will be given as

$$\frac{A_1}{B_1} \approx \left(\frac{v_c}{N_A \sigma^3}\right)^2 \tag{10}$$

In Table IV, the values of A_1/B_1 for nitrogen [1], methane [3], and mercury are compared with $(v_c/N_A\sigma^3)^2$ from the Lennard–Jones potential [15, 16]. The agreements are not exact but close enough to show the plausibility of the relation.

It is of interest to note that the density of the common compressibility factor point is predicted [3] to be at $\rho_{OZ}^2 = A_1/B_1$. The position of the common compressibility factor point can also be related to that of the common bulk modulus point [17]. Thus the position of these two points can also be used in comparison of the intermolecular potential parameters.

Table IV. Values of the Ratio A_1/B_1 from the Plots of $(Z-1)(v/v_c)^2 = A + B(\rho/\rho_c)^2$ Along with $[v_c/(N_A\sigma^3)]^2$ Values Predicted from the Lennard–Jones Potential

Fluid	A_1/B_1	$[v_c/(N_A\sigma^3)]^2$
N_2	9.0 ± 0.3[a]	8.07[b]
CH_4	7.33[c]	9.42[b]
Hg	8.06 ± 0.04[d]	7.45[e]

[a] Using data from Ref. 1.
[b] From Ref. 15.
[c] From Ref. 3.
[d] From the present work.
[e] Using $v_c = 40.1\ \text{cm}^3 \cdot \text{mol}^{-1}$ and data from Ref. 16.

8. DISCUSSION

The range of fluids to which the linear isotherm regularity can be applied has been extended in this paper. As mentioned, the regularity can also be seen as a simple three-parameter equation of state. Considering the range of high densities for which this equation is valid, it can provide a complement to the other, more familiar equations of state which are appropriate in the lower density regions of the phase diagram.

Having an analytical equation of state, of course, provides any number of applications, such as simple representation of experimental thermophysical data, calculation of thermodynamic functions, and use in engineering calculations.

The results obtained for hard-sphere and Lennard–Jones fluids show the general validity of the arguments proposed for the regularity. At the same time, it can be seen that expressing the behavior of these fluids in terms of the regularity can provide insight in regard to the physical factors operating in these systems.

Of the two real systems studied in this paper, mercury obeys the regularity excellently. Thus the scope of the regularity may be extended to include liquid metals.

For semiquantitative results, the regularity can be used for water, over a large pressure range. If the range of pressure is decreased, quantitative agreement can even be obtained for water.

Systems to which the regularity could be applied are other molten metal systems, including molten alloys. Molten salts, and in general electrolytic solutions, have also yet to be studied.

ACKNOWLEDGMENTS

The helpful comments and suggestions of Professor R. F. Snider and a number of other faculty and co-workers at the Department of Chemistry, University of British Columbia, are gratefully acknowledged. The author would also like to thank Professor G. A. Parsafar for providing some unpublished material. Finally, the author thanks the University of British Columbia for a University Graduate Fellowship.

REFERENCES

1. G. A. Parsafar and E. A. Mason, *J. Phys. Chem.* **97**:9048 (1993).
2. G. A. Parsafar and E. A. Mason, *J. Phys. Chem.* **98**:1962 (1994).
3. B. Najafi, G. A. Parsafar, and S. Alavi, *J. Phys. Chem.* **99**:9248 (1995).
4. S. Alavi, G. A. Parsafar, and B. Najafi, *Int. J. Thermophys.* **16**:1421 (1995).
5. M. Kac, G. E. Uhlenbeck, and P. C. Hemmer, *J. Math. Phys.* **4**:2711 (1963).

6. G. Ihm, Y. Song, and E. A. Mason, *J. Chem. Phys.* **94**:3839 (1991).
7. J.-P. Hansen and I. R. McDonald, *Theory of Simple Liquids*, 2nd ed. (Academic Press, London, 1986), p. 95.
8. J.-P. Hansen and L. Verlet, *Phys. Rev.* **184**:151 (1969).
9. J. O. Hirschfelder, C. F. Curtiss, and R. B. Bird, *Molecular Theory of Gases and Liquids*, 2nd printing (Wiley, New York, 1964), p. 1114.
10. I. R. McDonald and K. Singer, *Mol. Phys.* **23**:29 (1972).
11. L. Verlet and J.-J. Weis, *Phys. Rev. A* **5**:939 (1972).
12. H. S. Kang, C. S. Lee, T. Ree, and F. H. Ree, *J. Chem. Phys.* **82**:414 (1985).
13. T. Grindley and J. E. Lind Jr., *J. Chem. Phys.* **54**:3983 (1971).
14. G. A. Parsafar and N. Sohraby, *J. Phys. Chem.* **100**:12644 (1996).
15. D. A. McQuarrie, *Statistical Mechanics* (Harper and Row, New York, 1976), p. 244.
16. Y. Song and E. A. Mason, *J. Chem. Phys.* **91**:7840 (1989).
17. Y.-H. Huang and J. P. O'Connell, *Fluid Phase Equil.* **37**:75 (1987).